

Rocking motion induced charging of C_{60} on h -BN/Ni(111)

M. Muntwiler¹, W. Auwärter¹, A.P. Seitsonen², J. Osterwalder¹ and T. Greber¹

¹*Physik-Institut, Universität Zürich,*

Winterthurerstrasse 190, CH-8057 Zürich, Switzerland and

²*Institut für Physikalische Chemie, Universität Zürich,*

Winterthurerstrasse 190, CH-8057 Zürich, Switzerland

Abstract

One monolayer of C_{60} on one monolayer of hexagonal boron nitride on nickel is investigated by photoemission. Between 150 and 250 K the work function decreases and the binding energy of the highest occupied molecular orbital (HOMO) increases by ≈ 100 meV. In parallel, the occupancy of the, in the cold state almost empty, lowest unoccupied molecular orbital (LUMO) changes by 0.4 ± 0.1 electrons. This charge redistribution is triggered by onset of molecular rocking motion, i.e. by orientation dependent tunneling between the LUMO of C_{60} and the substrate. The magnitude of the charge transfer is large and cannot be explained within a single particle picture. It is proposed to involve electron-phonon coupling where C_{60}^- polaron formation leads to electron self-trapping.

PACS numbers: 81.05.Tp, 71.30.+h, 79.60.JV, 31.15.Ew

In the emerging field of molecular electronics C_{60} plays a pivotal role for the exploration and the test of new concepts. The separation of energy scales in inter- and intramolecular bonding gives rise to structural phase transitions that leave C_{60} intact. This is e.g. seen with diffraction experiments where orientational ordering of C_{60} was inferred from changes of the unit cell size [1, 2, 3]. Furthermore, C_{60} compounds have narrow electron bands [4], large on-site Coulomb repulsion and intramolecular phonons whose frequencies compare with the intermolecular electron hopping rates. The observation of high T_c superconductivity in alkali metal doped fullerenes [5] or antiferromagnetism [6] emphasizes strong correlation effects. On this background a rich variety of thermodynamic phases emerges where in view of applications metal insulator transitions are particularly interesting.

Here we report on the change of charge state of C_{60} that occurs in parallel to an orientational order-disorder transition. The underlying substrate of the C_{60} monolayer plays a crucial role: It provides the charge by tunneling, and it does not bind the C_{60} molecules strongly. h -BN/Ni(111) is an ultimately thin, atomically flat, metal-insulator interface. Its geometry and electronic structure is well known from experiments [7, 8] and density functional theory [9]. Compared to C_{60} /metal interfaces [10, 11], the substrate-induced doping, i.e. charge transfer on C_{60} , is much lower which allows to investigate the insulator limit. For the description of the C_{60}/h -BN/Ni(111) junction we borrow concepts from non-adiabatic gas surface reactions [12]. Charge transfer onto a molecule occurs when the vertical affinity level is degenerate with the Fermi level of the substrate. Provided that the tunneling electron resides long enough on the molecule, the molecule evolves towards its new equilibrium coordinates, i.e. approaches the adiabatic affinity level. The electronic system has to pay the energy for this Jahn-Teller distortion and can therefore not be described in a one-electron picture.

The experiments were performed in a modified VG ESCALAB 220 photoelectron spectrometer [13] with an attached scanning tunneling microscopy (STM) chamber [14]. The h -BN/Ni(111) interfaces were produced using the recipe by Nagashima et al. [7, 8]. C_{60} monolayers were prepared by annealing multilayers. On a linear heating ramp (0.15 K/s) C_{60} desorbs from the multilayer at 475K and from the monolayer at 520K. From this it is inferred that C_{60} is weakly bound on h -BN/Ni(111) (≈ 1.5 eV) [15]. At room temperature C_{60} wets the substrate and forms a commensurate hexagonally close packed (4 x 4) structure with a C_{60} nearest neighbor distance of 10.0 Å (see Figure 1). The STM picture in Figure

1b) shows how perfect the C_{60} /*h*-BN/Ni(111) junction grows.

Figures 1 c) and d) are low energy electron diffraction (LEED) data ($E = 23.5\text{eV}$) at 250 and 160 K, respectively. From comparison of the two it is seen that the unit cell size increases from a (4x4) with one C_{60} molecule to a quasi ($4\sqrt{3}\times 4\sqrt{3}R30^\circ$) unit cell with 3 C_{60} molecules when the sample is cooled to 160K. This is in line with the findings of Benning et al. [2] and Goldoni et al. [3], who found for C_{60} multilayers in the same temperature range a (1x1) to (2x2) surface lattice transformation. This phase transition corresponds to an order disorder transition which occurs in bulk C_{60} at $\approx 250\text{K}$ [1].

In Figure 2 He I α normal emission photoemission spectra for 300 and 160 K are shown. Due to the small mean free path of the photoelectrons the molecular orbitals of C_{60} dominate the spectra and the underlying substrate contributes only weakly. The bump at 0.6 eV binding energy reflects the Ni *d*-band. The C_{60} derived features are strongly temperature dependent. The highest occupied molecular orbital (HOMO) shifts from 2.75 up to 2.64 eV in going from 250 K to 160 K. Furthermore, the orbital peaks sharpen and the HOMO increases in intensity. From the large HOMO binding energy and the fact that there is no strong LUMO contribution which would produce a peak at the Fermi level we see that this system is an example for poor screening, i.e. high on-site Coulomb repulsion or large HOMO-LUMO separation in photoemission [10]. The work function increases parallel to the HOMO-shift from 4.25 to 4.37 eV. This indicates a charge redistribution in the interface and that the molecular orbitals are mainly bound to the vacuum level.

The inset of Figure 2 shows the spectra in the vicinity of the Fermi level. Intriguingly, a 80 meV down shift of the leading edge of the photoemission is observed in going from room temperature to 160 K. Such a shift is beyond instrumental uncertainties since the energy resolution was better than 60 meV. A careful comparison with the Fermi edge as measured on a Ag polycrystal indicates that the room temperature leading edge lies above E_F . As we show below it reflects a shift of the high binding energy wing of the LUMO parallel to the HOMO. The difference between the room temperature and the 160 K spectrum in the inset of Figure 2 corresponds to 4.5 % of the HOMO intensity at 300 K. This intensity can be assigned to the charge difference on the LUMO at high and low temperature, respectively.

To get a more quantitative measure of the LUMO occupancy a one parameter fit was applied to the data. The fit procedure asserts the same Gaussian spectral shape as that of the HOMO and a degeneracy-derived weight of 10 for the h_u HOMO and 6 for a fully occupied t_{1u}

LUMO [16]. The Gaussian for the LUMO is fitted to the spectrum that was divided by the corresponding experimental Fermi function (see inset of Figure 3). The only fit parameter is the HOMO-LUMO energy difference [17], and the fit is performed in a region from the Fermi energy up to 200 meV above E_F . In order to obtain the LUMO occupancy the Gaussian for the LUMO is multiplied with the Fermi function and integrated. Figure 3 shows this LUMO occupancy versus the reciprocal temperature. It increases by a factor of 7 ± 1 in going from 150 to 300 K [18]. Though these data are recorded during cool down of the sample, the effect is reversible with a hysteresis < 50 K. From the fit the LUMO occupancy changes between room temperature and 160 K by \approx half an electron. This is in good agreement with 0.45 electrons [19] as independently derived from the difference of the spectra near the Fermi energy (inset of Figure 2) and the comparison with the HOMO intensity. In Figure 3 we show as well the intensity of the HOMO. It decreases in a non Debye-Waller fashion with increasing temperature and indicates changes in molecular orientation as reflected in ultraviolet photoelectron diffraction (UPD) [20]. The transition temperature coincides with that of the change in charge state. This is a clear indication that the charge state is closely related to the molecular orientation. Since the spectra were recorded in normal emission it can be inferred that the change in orientation must contain rocking motion, i.e. rotational axes that do not coincide with the surface normal.

How can we explain the change in charge transfer with temperature? In Bardeen's tunneling picture the charge transfer between the substrate and the adsorbate is related to the overlap of the wave functions at the Fermi level [21]. The charge on the C_{60} molecules thus reflects a finite tunneling probability of conduction electrons across the h -BN layer onto the LUMO of C_{60} . The residual occupancy of 0.08(2) electrons at low temperatures indicates that electron tunneling from the substrate to the molecule is still enabled, though at a low rate. At temperatures above 250 K the charge transfer begins to saturate. From this non Arrhenius behavior a model where the charge transfer is induced by thermally excited electrons alone, has to be refuted. However, the increase of the LUMO occupancy with temperature is related to the onset of molecular rocking motion in the C_{60} monolayer (see Figure 3) and therefore a molecular orientation dependent wave function overlap with the substrate gives a natural explanation for the effect. The onset of molecular rocking motion is in line with the known disorder transition in C_{60} multilayers [2, 3], the LEED patterns in Figure 1, X-ray photoelectron diffraction (XPD) and Ultraviolet Photoelectron Diffraction (UPD)

(also see Figure 3) patterns. Furthermore, the XPD patterns (not shown) indicate that the C_{60} molecules do not bind via the pentagons but rather via hexagons to the substrate, as it is e.g. the case for C_{60} on Cu(111) [22].

In order to justify the molecular rocking driven model, the electronic structure of C_{60} has to deviate from spherical symmetry. For this purpose density functional calculations were performed within the Kohn-Sham scheme. As the exchange correlation functional we employed the Generalized Gradient Approximation (GGA) of Perdew, Burke and Ernzerhof [23]. The Kohn-Sham orbitals were expanded either in a Gaussian basis set TZVP in the TURBOMOLE code [24] or in plane waves with a cutoff energy of 40 Ry. In the latter case the action of the core electrons on the valence electrons was replaced with norm-conserving pseudo potentials, and the length of the supercell was 21.2 Å.

Figure 4 shows results of density functional calculations of C_{60} . In Figure 4a) the degenerate LUMO is shown as a constant electron density isosurface. Clearly, the LUMO electron density is largest on the pentagons, while the hexagons have a low density. Together with the fact that at low temperatures C_{60} does not expose pentagons towards the substrate this gives a consistent picture: The overlap between the LUMO and the substrate, i.e. the tunneling rate increases if the molecules rock away from the equilibrium position and correspondingly more electrons tunnel into the LUMO. This overlap is shown in Figure 4b) as a function of the molecular orientation relative to the surface normal. The grey scale plot gives the integral of the LUMO in the half space $z > z_o$ with $z_o = 5\text{Å}$ away from the center of C_{60} as a function of the molecular orientation relative to this plane. The average probability to find an electron outside a plane $z > z_o$ i.e. the mean of the integrals over all orientations $\int |\Psi_{LUMO}(z > z_o)|^2$ is $0.007 \int |\Psi_{LUMO}|^2$ and the anisotropy that we call tunneling anisotropy may be seen in the bottom panel of Figure 4b). The tunneling anisotropy slightly depends on z_o , though for reasonable $z_o \geq 5\text{Å}$ it never reaches values that could explain quantitatively the strong temperature dependence of the LUMO occupancy. From the experiment the LUMO occupancy ratio between room temperature and low temperature is ≈ 7 , while a tunneling anisotropy of 0.75 could explain a ratio of 1.3 only. In other terms this theory explains an occupancy change of 0.01 electrons only, which is inconsistent with observation.

Thus we have to refine the orientation dependent tunneling picture. It is unlikely that the substrate wave function and/or distance induced changes in the tunneling matrix element account for the strong *amplification* of the effect. Also, electron hopping between the C_{60}

molecules is not expected to change the net charge balance in such a dramatic way. It is rather an indication that the one-electron picture as it is drawn from the tunneling anisotropy in Figure 4b) breaks down. The low tunneling rate provides substantial time for an electron to stay and to act on the C_{60} layer before it returns to the substrate. For large residence times, comparable with the molecular vibration periods, the C_{60}^- species start to deform and the electron couples strongly to phonons. In other terms, C_{60}^- distorts from the vertical affinity E_A^V towards the adiabatic affinity E_A^A . Our calculations on gas-phase C_{60}^- result in a Jahn-Teller distortion energy, i.e. energy difference between unrelaxed and relaxed C_{60}^- $E_A^V - E_A^A$ of 51 meV. In the condensed phase we have to consider intramolecular *and* extramolecular vibrations. Though, their interplay and relative importance is not known at the moment. Intramolecular electron phonon coupling is e.g. observed in photoemission from C_{60}^- [25], or recently in inelastic tunneling experiments on $C_{60}/\text{Ag}(110)$, where an electron energy loss of 54 meV was assigned to the excitation of a H_g phonon [26]. Near metallic surfaces the coupling to extramolecular vibrations occurs via the image force on the C_{60}^- ion, which excites frustrated translational vibrations. In this image field the occupied LUMO dives below the Fermi level and gets trapped since back-tunneling to the substrate is prevented due to the lack of empty states. Together with the onset of Coulomb repulsion this may establish a new equilibrium LUMO occupancy. If indeed such a kind of ‘polaron’ driven self trapping mechanism is responsible for the strong amplification of the tunneling anisotropy this is a particular example for strong electron phonon coupling in such an interface system.

In summary we report the observation of a temperature driven change in C_{60} molecular orbital binding energies parallel to the work function and a strong change in LUMO occupancy of C_{60} on $h\text{-BN}/\text{Ni}(111)$ that coincide with the onset of molecular rocking. The charge transfer is triggered by an anisotropic tunneling matrix element of the C_{60} LUMO with the underlying substrate. The magnitude of the charge transfer is an indication for strong electron-phonon interactions. This effect might open the door for the application of the orientation dependence of the tunneling across molecules for electronic and spintronic switches.

Fruitful discussions with F. Baumberger and R. Monnier and funding from the Schweizerischen Nationalfonds is gratefully acknowledged.

-
- [1] P.A. Heiney, J. E. Fischer, A.R. McGhie, W.J. Romanow, A.M. Denenstien, J.P. McCauley Jr., A.B. Smith and D.E. Cox, Phys. Rev. Lett. **66** (1991) 2911.
- [2] P.J. Benning, F. Stepniak and J.H. Weaver, Phys. Rev. B, **48** (1993) 9086.
- [3] A. Goldoni, C. Cepek and S. Modesti, Phys. Rev. B, **54** (1996) 2890.
- [4] W.L. Yang et al., Science **300** (2003) 303.
- [5] A.F. Hebard et al. Nature **350** (1991) 600.
- [6] T. Takenobu, T.Muro, Y. Iwasa, T. Mitani, Phys. Rev. Lett. **85** (2000) 381.
- [7] A. Nagashima, N. Tejima, Y. Gamou, T. Kawai and C. Oshima, Phys. Rev. Lett. **75** (1995) 3918.
- [8] W. Auwärter, T.J. Kreutz, T. Greber and J. Osterwalder, Surf. Sci. **429** (1999) 229.
- [9] G. B. Grad, P. Blaha, and K. Schwarz, W. Auwärter and T. Greber, Phys. Rev. B **68** (2003) 085404.
- [10] P. Rudolf, M.S. Golden, P.A. Brühwiler, J. Electron Spectros. and Rel. Phen. **100** (1999) 409.
- [11] M. Kiguchi, K. Izumi, K. Saiki and A. Koma, Appl. Surf. Sci. **212-213** (2003) 101.
- [12] T. Greber, Surf. Sci. Rep. **28** (1997) 3.
- [13] T. Greber, O. Raetzo, T. J. Kreutz, P. Schwaller, W. Deichmann, E. Wetli and J. Osterwalder, Rev. Sci. Instrum. **68** (1997) 4549.
- [14] W. Auwärter, M. Muntwiler, J. Osterwalder and T. Greber, Surf. Sci. **545** (2003) L735.
- [15] P.A. Redhead, Vacuum **12** (1962) 203.
- [16] This LUMO weight is supported by a HOMO:LUMO intensity ratio of 10:6 at 21.1 eV photon energy in K_6C_{60} on Ag(100). C. Cepek, M. Sancrotti, T. Greber and J. Osterwalder, Surf. Sci. **454-456** (2000) 467.
- [17] The HOMO-LUMO energy difference remains constant (≈ 3.1 eV) and is close to the value of undoped C_{60} .
- [18] The HOMO:LUMO intensity ratio may depend on the molecular orientation. If it changes by a unrealistically large factor of 2, we would expect the LUMO occupancy to change by a factor of 3 instead of 7.
- [19] Four independent experimental runs gave an average charge difference of 0.35 ± 0.08 electrons between low temperature and room temperature.

- [20] J. Osterwalder, T. Greber, P. Aebi, R. Fasel and L. Schlapbach, Phys. Rev. B, **53** (1996) 10209.
- [21] J. Bardeen, Phys. Rev. Lett. **6** (1961) 57.
- [22] R. Fasel, P. Aebi, R.G. Agostino, D. Naumović, J. Osterwalder, A. Santaniello and L. Schlapbach, Phys. Rev. Lett. **76** (1996) 4733.
- [23] J. P. Perdew, K. Burke, and M. Ernzerhof, Phys. Rev. Lett. **77** (1996) 3865; *ibid.* **78** (1997) 1396; *ibid.* **80** (1998) 891.
- [24] R. Ahlrichs, M. Bär, M. Häser, H. Horn, and C. Külmel, Chem. Phys. Lett. **162** (1989) 165: see <http://www.turbomole.de/>
- [25] O. Gunnarsson, H. Handschuh, P.S. Bechthold, B. Kessler, G. Ganteför and W. Eberhardt, Phys. Rev. Lett. **74** (1995) 1875.
- [26] J.I. Pascual, J. Gómez-Herrero, D. Sánchez-Portal and H.-P. Rust, J. Chem. Phys. **117** (2002) 9531.

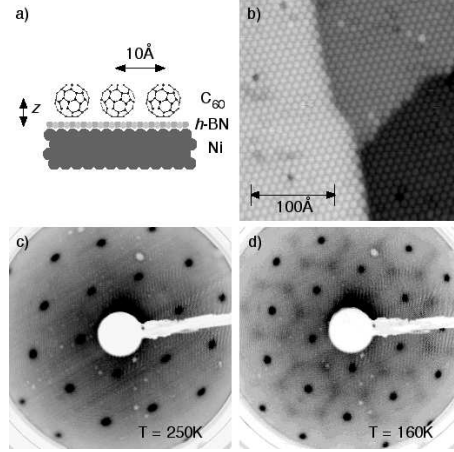


FIG. 1: The investigated system $C_{60}/h\text{-BN}/\text{Ni}(111)$. a) Sketch of the interface. b) STM picture of the well ordered monolayer of C_{60} . The three grey levels indicate three different terraces on the substrate. c,d) LEED patterns ($E = 23.5\text{eV}$): (4×4) at 250K and quasi $(4\sqrt{3}\times 4\sqrt{3})R30^\circ$ at 160K.

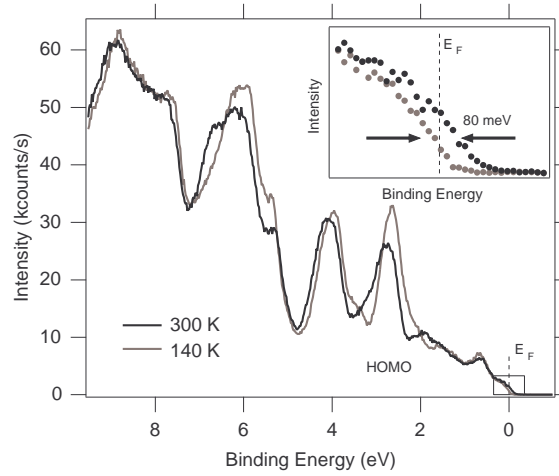


FIG. 2: He $I\alpha$ photoemission spectra of one monolayer of C_{60} on $h\text{-BN}/\text{Ni}(111)$ for room temperature and 160 K. The inset shows the strong shift of the photoemission leading edge that is due to the population of the LUMO at high temperatures.

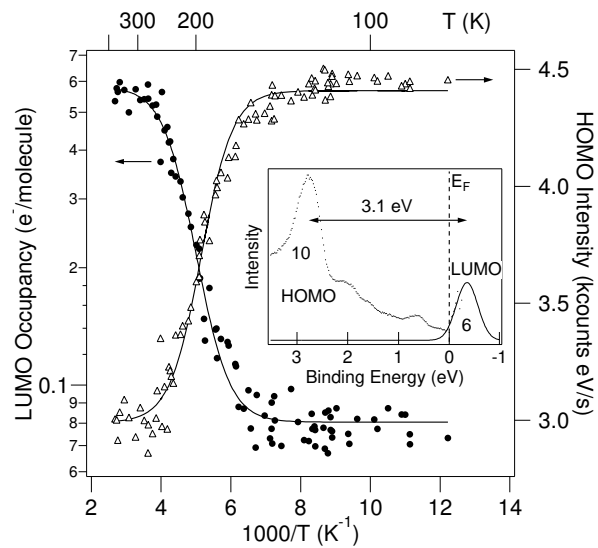


FIG. 3: Occupancy of the LUMO (solid circles) and normal emission HOMO intensity (open triangles) as a function of reciprocal temperature. The solid lines are guides to the eye. The inset shows the extrapolated LUMO from the 300 K data in Figure 2.

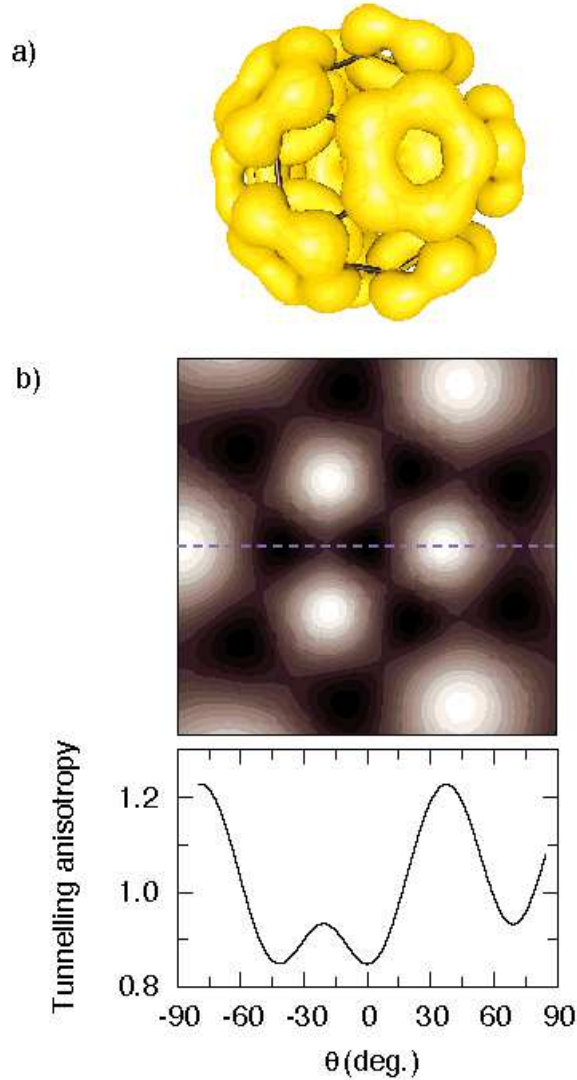


FIG. 4: Deviation of the LUMO of C_{60} from spherical symmetry. a) Constant electron density isosurface. b) Stereographic projection of the integral electron density outside planes placed 5 \AA away from the center of C_{60} . The low density parallel to hexagons (center of the plot) and the high density parallel to pentagons is apparent. The bottom panel shows the anisotropy of this electron density that is related to the tunneling rate between the substrate and the molecule along the dashed θ line. The tunneling anisotropy of 1 corresponds to the average of all molecular orientations.